PHYSICAL REVIEW B VOLUME 19, NUMBER 6 15 MARCH 1979

Transmission, photoconductivity, and the experimental band gap of thermally grown SiO_2 films

Z. A. Weinberg,* G. W. Rubloff, and E. Bassous
IBM Thomas J. Watson Research Center, P. O. Box 218, Yorktown Heights, New York 10598
(Received 10 October 1978)

Optical transmission and photoconductivity spectra (7–14 eV) and the field dependence of photoconductivity are presented for thermally grown (amorphous) SiO_2 films. It is argued that the clearest experimental determination of the band gap in SiO_2 can be obtained from the field dependence of photoconductivity and its similarity to internal photoemission; a band gap of 9.3 eV for amorphous SiO_2 is deduced from the data. In view of this result some recent experimental band-gap determinations are criticized and the literature on this subject is examined. The transmission experiments were performed on thin thermally grown (amorphous) SiO_2 films (450–5000 Å) produced by etching off the silicon substrate and using a fabrication method which is described in detail. The photoconductivity measurements were performed on Al-SiO_2-Si structures (SiO_2: 600–3500 Å). Diode experiments for detecting photoluminescence and possibly excitons are also described. The upper limit on photoluminescence yield was determined as $\sim 10^{-4}$.

I. INTRODUCTION

The experimental determination of the band gap of SiO_2 is a difficult task because of its long absorption tail and the presence of exciton effects in its optical spectra. It is not surprising, therefore, that the experimental band gap is found to vary quite widely in the literature. In this paper we review the subject and propose that the field dependence of photoconductivity can be used to deduce a band gap of 9.3 eV for SiO_2 (Ref. 1) (for more discussion of this value see Sec. III). This method is quite different from the conventional procedure of extracting a threshold from spectral data, a procedure which is subject to many complications as is explained throughout Sec. II. This section also describes in some detail our measurements on transmission and photoconductivity of thermally grown SiO_2 films.

In spite of the considerable attention devoted to studies of SiO_2, the character of its band gap remains unresolved both experimentally and theoretically, and its experimental value is found to vary anywhere from 5 to 12 eV in recent literature.[2-4] In order to further illuminate this issue, we present below a review of the experimental values of the band gap, found scattered in the literature, including the newer results which are not confirmed by our data. On the theoretical side, Griscom[5] has published an excellent review of the electronic structure of SiO_2 and its spectroscopic aspects; an elegant summary of theoretical advances has been offered by Pantelides[6]; for more recent advances the reader is referred to Ref. 7. For the sake of completeness we shall mention here, only briefly, the recent theoretical predictions regarding the SiO_2 band gap. Mott, in his review article,[8] estimated the band gap to be at about 10.6 eV, i.e., above the first peak in the optical spectra (10.45 eV in Fig. 4); however, he has since accepted the view that the band gap is at about 9 eV (largely on the basis of the data presented in this paper and in Ref. 1), and he proposes that it is indirect with the 10.45-eV peak being a direct gap exciton[9] (presumably below a higher-lying direct gap). Chelikowski and Schlüter's band-structure calculation[10] for crystalline α-quartz yielded an indirect band gap of 9.2 eV and the lowest direct gap was found to be 9.8 eV.[11] Schneider and Fowler[12] and Calabrese and Fowler[13] find the band gap to be direct forbidden. Ciraci and Batra[14] have computed a direct gap at 9.8 eV for the idealized form β-cristobalite. While all the above band-structure calculations neglect the important electron-hole interaction, it has been incorporated into the calculation of the optical absorption spectrum for the first time by Pantelides,[15] who finds that electron-hole interactions have a strong effect so that excitonic peaks dominate the entire spectrum.

One of the earliest measurements of absorption in quartz (extended to 8.44 eV) was reported by Groth and Weyssenhoff,[16] and their data was the basis for Williams' band-gap estimation of 8 eV.[17] Photoemission of holes from silicon into thermally grown SiO_2 was reported by Goodman,[18] with the energy difference between the conduction-band edge in the silicon and the valence-band edge in the oxide given by about 4.9 eV. This yields a band gap of 8.0–8.1 eV when combined with the energy difference between the conduction-band edges of silicon and SiO_2, which has been much more firmly established at 3.1–3.2 eV.[19,20] The earliest reflectance spectrum of SiO_2 (in the form of natural brazilian quartz) was reported by Loh[21]; he identified the

first spectral peak (~10.4 eV) as excitonic and crudely estimated the band gap to be above it, at about 11 eV. The excitonic assumption was further strengthened by the observation of Platzöder,[22] on α-quartz, that the first two reflectance peaks are temperature dependent. More refined reflectance spectra of crystalline and fused (amorphous) quartz were published by Philipp.[23,24] Although Philipp did not attempt to estimate the band-gap energy from his spectra, Powell and Derbenwick[25] used Philipp's results to conclude that the fundamental absorption edge of SiO_2 is at approximately 9 eV. In the same paper[25] the authors suggest a band gap of 8.8 eV from their measurements of hole trapping in thermally grown SiO_2 films illuminated by vacuum-ultraviolet (vuv) photons.

Until recently, the most accepted band-gap value was due to DiStefano and Eastman,[26] who determined an interband gap of 9.0 eV by fitting their photoconductivity spectra (performed on a 5000-Å thermally grown SiO_2 film) to a parabolic absorption-edge characteristic of an indirect gap. They also determined a band gap of 8.9 ± 0.2 eV from photoemission of electrons from SiO_2 into vacuum (for which they place the threshold at 10.2 eV) and similarly from silicon through 150 Å of SiO_2 into vacuum (for a review of these results see Ref. 5). We note in passing that the 8.9-eV value would be revised upward to 9.3 eV if one assumes that the valence-band edge of SiO_2 lies at 10.6 eV below vacuum, as indicated by Ibach and Rowe[27] from electron energy-loss spectroscopy measurements on thermally grown SiO_2 films.

In contrast to the above trend, the region for creation of electron-hole pairs has been placed much higher (above 12 eV) by Zakis *et al.*[28] (see also Trukhin, below)—and on the other hand much lower band-gap values were proposed by Stephenson and Binkowski.[2] The latter authors observed a soft shoulder in their x-ray photoelectron spectroscopy (XPS) data obtained on α-quartz and fused silica, but this was absent in OH-rich silica glass. They propose the following lower and upper limits on the SiO_2 band gap: 5.55–7.8 eV for α-quartz, 5.05–7.3 eV for fused silica, and up to 8.3 eV for OH-rich silica. These results have already been criticized by Griscom[5] on the basis of defects introduced in the surface of the sample during its preparation by vacuum milling. We add here that such low band-gap values would imply unreasonably low barriers for hole injection from the electrodes into SiO_2 in metal-oxide-silicon (MOS) structures. These have not been observed although such low barriers would have been easily seen because holes conduct quite readily in SiO_2 at room temperature.[29,30] Interestingly, in contrast to Stephenson and Binkowski, Kaminow *et al.*[31] find that the absorption edge of their dry silica occurs at an energy 0.2 eV higher than for their wet silica.

More recently, Trukhin[4] published photoconductivity spectra of crystalline quartz, fused silica, and thermally grown SiO_2 films on silicon. For all his samples the data show an exponential rise from about 8.8 eV with some rounding observed above 12 eV (Fig. 5 in Ref. 4). Trukhin interprets his data as evidence for a direct band gap of 12 eV and a lowest band gap of 9.5 eV. Trukhin's photoconductivity spectra and likewise the earlier photoconducitvity results of Zakis *et al.*[28] are completely inconsistent with our results (see Fig. 7) and those of DiStefano and Eastman.[26] Appleton *et al.*[32] have measured transmission and photoconductivity of α-quartz and vitreous SiO_2, and suggest, following Mott,[8] a direct band gap of 10.6 eV with the possibility of a lower indirect band gap of about 9 eV.

In a more elaborate band-gap determination Powell and Morad[3] obtain a value of 8.0 ± 0.2 eV, which is the same threshold they find in the absorption coefficient, photoconductivity spectra, and positive charging effects of thermally grown SiO_2 films. We find ourselves in disagreement with this result. First, the thresholds in these spectra cannot be determined very accurately because of interference and internal photoemission effects, as is described in Sec. II; second, the threshold of spectral data may not represent the band gap, as is explained in Sec. III.

In addition to the above literature, many papers have dealt with the optical absorption edge of various glasses, which is generally sensitive to impurities and radiation damage. References on these subjects can be found in the reviews by Sigel[33] and Lell *et al.*[34]

II. EXPERIMENTAL RESULTS

Initially, the transmission experiments (Sec. IIA) and photoconductivity measurements (Sec. IIB) were motivated by the need for accurate data on the optical absorption coefficient and on electron-hole separation in SiO_2 to supplement our experiments on the possibility of exciton migration.[1,35] It developed that our results did not confirm the band-gap determination presented in recent publications,[2-4] and therefore, we shall emphasize in this section the points of disagreement and the difficulties in extracting a threshold from the spectral data. Instead, we propose that the field dependence of photoconductivity (Sec. IIC) may be a better means for band-gap de-

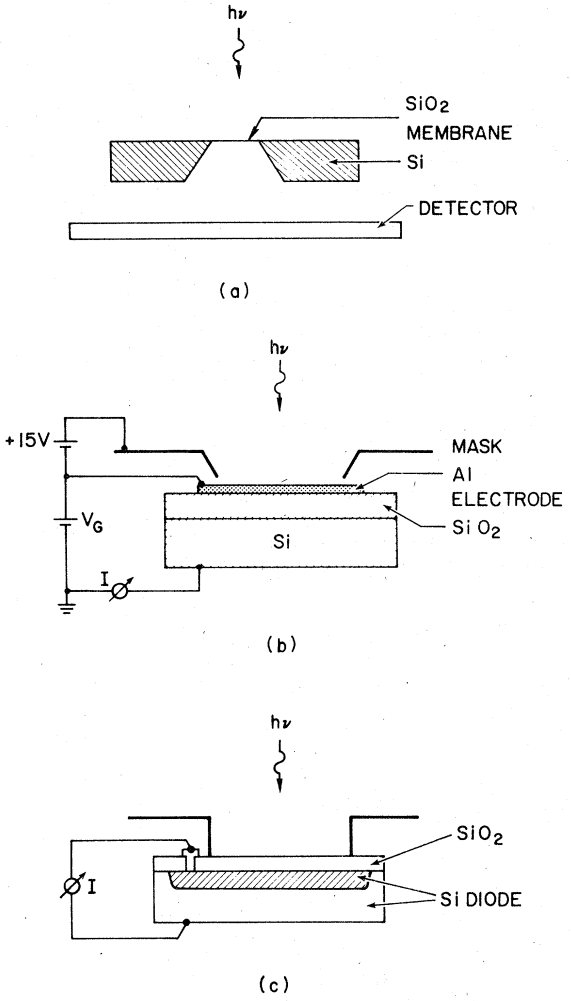

FIG. 1. (a) Schematic illustration of the transmission experiment with thin SiO_2 membranes. The detector was a sodium salicylate coating which converts the incident vuv light ($h\nu$) to lower energy photons detected by a photomultiplier. (b) Schematic illustration of the photoconductivity experiments on mos structures. The contact leading to the current meter (I) was completely shielded from secondary photoemitted electrons by the sample housing (not illustrated), and by the mask which also shields the unmetallized surface of the oxide. V_G was negative (Al side) for the data of Figs. 6–9. (c) Schematic illustration of the diode experiments for transmission, photoluminescence, and exciton detection.

termination.

The three device structures used in our study are illustrated schematically in Fig. 1. Thin oxide membranes [Fig. 1(a)] were used for transmission measurements, MOS structures [Fig. 1(b)] were employed for photoconductivity studies, and the diode structures [Fig. 1(c)] were used in an attempt to detect excitons and photoluminescence. More experimental details are found in the appropriate section below.

In each of the experimental arrangements the incident ultraviolet photon flux was monitored by the fluorescence of a sodium salicylate layer[36] which is assumed to have an approximately flat conversion efficiency of vuv to lower energy photons, which are then detected by a photomultiplier. Vuv light was obtained from a McPherson model 225 monochromator equipped with a H_2 discharge lamp and an AL/MgF_2-coated grating of 1200 lines/mm. The samples were mounted approximately 3 cm away from the monochromator's exit slit, which was open to 1.0 mm, giving a wavelength resoltuion of 8 Å (FWHM).

A. Transmission through thin oxide membranes

1. Membrane preparation

As described by Powell and Morad[3] (abbreviated herein as PM), thin oxide membranes produced

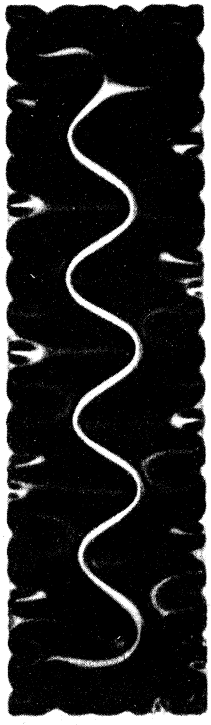

FIG. 2. Photograph of a membrane measuring 1.0 ×0.25 mm, showing the sinusoidal pattern produced by microscope light interference in the slightly wrinkled SiO_2 film.

by the anisotropic etching of silicon[37,38] can be used for measuring optical transmission. PM have used the simplest technique of membrane preparation where the initial thick oxide used as an etching mask is also the final oxide to be studied (reduced in thickness during the silicon etching). Although we have also tested this technique, a more elaborate fabrication method was adopted in order to retain better control over the processing and thickness of the final oxide. The technique employs a layer of Si_3N_4 for protection, as described below. Oxides, 400–600 Å thick, were thermally grown in dry O_2, steam, or dry O_2 with HCl (4.5%) ambients. These ultrathin membranes are suitable for measuring transmission in the strongly absorbing region of SiO_2 ($\gtrsim$10 eV). To extend the measurement to the less absorbing region, membranes with about 1000 Å and 5000 Å of dry oxide were also prepared. A photograph of a typical membrane is shown in Fig. 2. It was found that the elongated structure gives better support to the membrane and that the sinusoidal pattern produced by interference (due to the slight wrinkling of the film) is a good indication of the membrane integrity. These membranes have exhibited a remarkable resilience during final fabrication and handling steps. We proceed to describe the membrane preparation method in some detail since it includes a few novel steps.

Silicon wafers 57 mm in diameter, 0.4 mm thick, polished on one side, (100) oriented, 2–5 Ω cm p-type were thermally oxidized to a thickness slightly above the final desired value. The oxidation conditions investigated were: dry O_2 at 1000 °C, dry O_2 with 4.5% HCl at 1000 °C, and wet oxidation at 800 °C. The oxides were then coated with 1500 Å of chemical-vapor-deposited Si_2N_4 deposited from SiH_4 and NH_3 at 800°C. The purpose of the Si_3N_4 film is to protect the initial SiO_2 during the anisotropic etching of the silicon. A second wet oxidation was performed to grow 5000 Å of SiO_2 on the unpolished back side of the wafers. Using standard photolithography, a pattern of rectangular openings (1.42 × 0.81 mm) and a grid defining chip sizes were etched in the back side oxide with the pattern aligned parallel to the wafer flat or ⟨110⟩ direction. The silicon was then etched through this pattern by an anisotropic etching solution containing 12 g of pyrocatechol, 75 ml of ethylene diamine, 6 ml of H_2O_2 (30%), and 18 ml of water. At its boiling point of 118± 1 °C, the solution etches (100) silicon at about 130 μm/h, which is approximately twice the rate of the more commonly used etchant[39,40] without H_2O_2. Etched cavities were formed with the four convergent {111} walls inclined at 54.7° with respect to the wafer's surface. The wafers were removed from the etching solution when the etched silicon thickness reached 3–10 μm as determined by monitoring the membrane transparency under a microscope. To form the free SiO_2 membrane, the Si_3N_4 film was etched in boiling H_3PO_4 at 180 °C, followed by removal of the underlying thin silicon by the anisotropic etchant. The latter step was carefully controlled to minimize etching of the backside of the SiO_2. Since the etching rate of SiO_2 is slow (approximately 130 Å/h), we estimate that at most a 5-Å layer of SiO_2 might be removed in this step. The wafers were then separated into chips by breaking them along the grid lines defined by the etching. The yield of good membranes was about 20%. The oxide thickness (±1%) was measured by ellipsometry on each chip, adjacent to the membrane, after the transmission experiment was completed.

2. *Experimental results*

Several chips were mounted in a rotary holder, with their oxide side facing the light source, as shown schematically in Fig. 1(a). One of the chips had its oxide etched off to serve as a reference. The transmission data were obtained by dividing the oxide signal by the reference signal after each had been corrected for the scattered light contribution. Corrections for small differences in membrane sizes were done, initially by etching the oxide off and calibrating the aperture's transmission relative to the reference. Alternatively, a simpler procedure was adopted (which is probably more accurate), where the

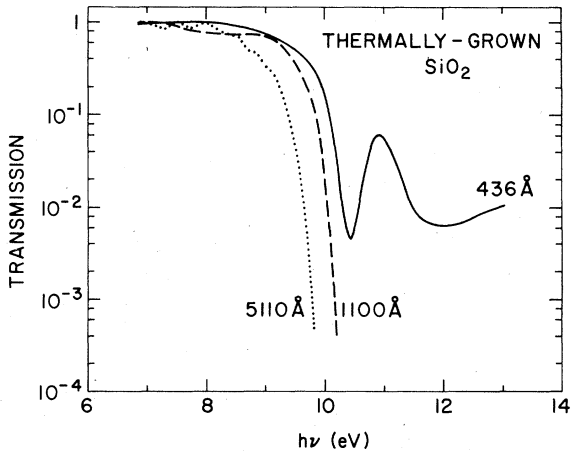

FIG. 3. Optical transmission data for three oxide thicknesses (for clarity, measured points are not indicated).

transmission was normalized to unity at the interference peak at low photon energies, which is the theoretical value for a transparent film. Such transmission data are shown in Fig. 3 for three oxide thicknesses of 436, 1100, and 5110 Å.

The absorption coefficient (α) was evaluated by an iterative procedure from the transmission (T) using the exact formula as described in Appendix A. In the calculation the initial values of k were taken from Philipp,[41] while his values of n were assumed throughout, where $n-ik$ is the complex index of refraction. For the range where $T<0.2$ the error resulting from the use of Philipp's data for n is small: a ±10% change in n yields a change of ±2% or smaller in α. The absorption coefficient is shown in Fig. 4 and the tail region is shown on an expanded scale in Fig. 5. Figure 4 gives a comparison between our results for a 436-Å SiO_2 film, Philipp's Kramers-Kronig analysis of fused silica reflectance data, and PM's results for a 580-Å SiO_2 film. We have found it necessary to shift Philipp's data by +0.075 eV to align the position of his first peak with ours and that of PM. It is not clear whether this small shift is due to a real difference between thermally grown SiO_2 and fused silica or to errors resulting from the Kramers-Kronig analysis. As seen in Fig. 4, good agreement is found between Philipp's data and our results over

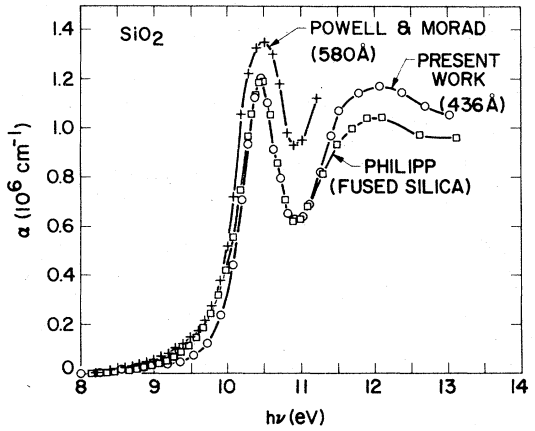

FIG. 4. Absorption coefficient of amorphous SiO_2 (for the expanded tail region see Fig. 5). The "present work" curve was calculated from the transmission data of Fig. 3, as explained in Sec. II A. Powell and Morad's curve was reproduced from Fig. 2 of Ref. 3. Philipp's curve was obtained from his optical constants (calculated by Kramers-Kronig analysis of reflectance data; see Ref. 41) and shifted by +0.075 eV to align the positions of the first peak (see text).

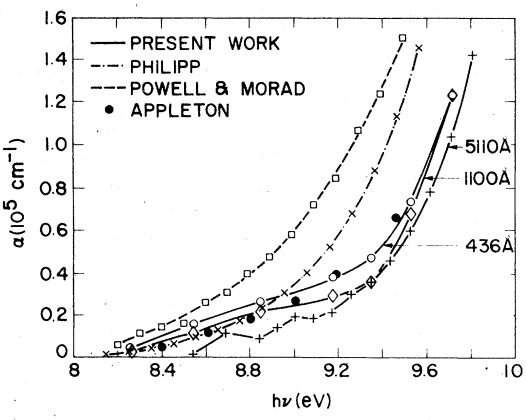

FIG. 5. Absorption tail region. Note the expanded scale of α. Our data is considered reliable only in the range of $h\nu > 9.2$ eV for the 5110-Å film; for lower $h\nu$, interference effects are clearly visible. A few points from Appleton *et al.* (Ref. 32) for vitreous SiO_2 are added for comparison.

an appreciable energy range. The discrepancy above about 11.5 eV might be due to the appreciable scattered light correction in our data in this region. The discrepancy below about 10 eV, again, is due to either real differences between the oxides or to errors in Kramers-Kronig analysis. The discrepancy between our result and that of PM is much larger than our experimental error and, in our opinion, cannot be explained by differences in oxide processing. The accuracy of α in our data is estimated to be better than ±2% for the region where $T<0.2$, which applies from about 9.2 eV for the 5110-Å film to about 11.3 eV for the 436-Å film. Above 11.3 eV the scattered light correction becomes appreciable and the error could be as high as 10%. The reproducibility of α among membranes of various oxide thicknesses and processing, as described in Sec. II A 1, has been within ± 5%.

The absorption tail region is shown in expanded scale in Fig. 5 and a few points from measurements on thin vitreous silica by Appleton *et al.*[32] are also shown. In our results it is evident that when the transmission approaches unity (Fig. 3) the errors in α become larger and interference effects cannot be entirely corrected by the use of Philipp's optical constants. Therefore, we consider our results to be reliable only down to about 9.2 eV for the 5110-Å film. Similarly, the Kramers-Kronig analysis of Philipp's data is also questionable in the tail region. The data of PM show much stronger absorption than even the data of Appleton *et al.* on vitreous SiO_2,

which is not reasonable considering the high purity of thermally grown SiO_2.

We conclude this section by remarking that the 8-eV threshold determined by PM (Fig. 2 in Ref. 3) from a square-root fit of the absorption tail seems very doubtful in view of the low reliability of the measurement in the absorption tail on ultrathin films, as discussed above.

B. Photoconductivity spectra

1. Experimental

MOS capacitors were mounted in a manner shown schematically in Fig. 1(b). The photocurrent flowing in the oxide was measured on the substrate side (I) and a mask was employed to shield the unmetallized regions of the SiO_2 and to collect secondary emitted electrons. The use of a mask is important since vuv light impinging on the exposed regions of the oxide will charge up these regions and cause current to flow through the oxide, resulting in erroneous current readings. Similarly, erroneous readings will occur if secondary photoemitted electrons can reach the contact region where the current is measured. The proper functioning of the mask has been verified by checking that varying the mask voltage did not affect the current readings, especially at low photon energies where the oxide currents are small. As a matter of routine the mask was held at +15 V with respect to the gate. An *in situ* calibration of the light intensity was obtained by rotating the sample holder away from the beam and using the same detection method as explained in the introduction to Sec. II.

The oxides were thermally grown on (100), 2-Ω cm p-type silicon wafers. Thicknesses up to about 1000 Å were prepared by a dry oxidation followed by 5-min anneal in an argon ambient. Higher thicknesses were prepared by a dry-wet-dry oxidation with a similar anneal, all done at 1000 °C. The wafers were all metallized together with a pattern of aluminum dots, 1.25 mm in diameter and about 160 Å thick. The contact was initially made on a thicker Al pad, but it was found that direct bonding to the thin Al is simpler and serves equally well.

2. Results and discussion

The spectral dependence of photoconductivity is shown in Fig. 6 for three oxide thicknesses of 575, 1015, and 2310 Å, with the region at low photon energies multiplied by 10 for clarity. As explained below, the tail also contains photocurrent contributions resulting from internal photoemission (IPE) from the aluminum. The

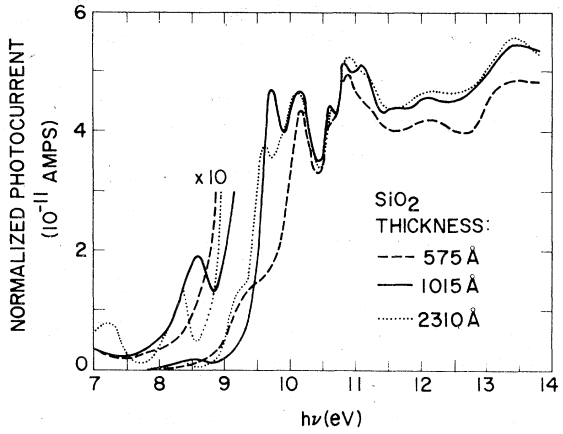

FIG. 6. Normalized photoconductivity spectra. The currents were normalized to the incident photon flux and the scale shown corresponds to the range of actual measurements. The data are not corrected for reflectance, which is the cause of most of the structure for $h\nu > \sim 10$ eV. For $h\nu < \sim 10$ eV, interference effects are clearly visible and in the tail region (expanded by 10) internal photoemission of electrons from the Al is appreciable. The data were taken with an average field of 2×10^6 V/cm across the SiO_2, with the Al biased negatively [$-V_G$ in Fig. 1(b)].

data shown are uncorrected for reflectance or interference effects. Such corrections were attempted but have been found inadequate, presumably because a three-layer structure requires a more precise knowledge of all optical constants.

The data of Fig. 6 show a more complete and a more complex behavior than previously published. Clearly, the determination of a threshold, or a band gap, from such data is difficult in view of the obvious strong interference effects and appreciable internal photoemission contribution at low photon energies. It is interesting to compare our results with the literature. DiStefano and Eastman[26] extracted a 9-eV band gap by fitting a portion of their photoconductivity data, obtained on a 5000-Å SiO_2 film, to a parabolic absorption law. However, we have determined that interference effects persist even for higher thicknesses (measurements were carried up to 3500 Å and absorption calculations up to 6000 Å); therefore, their fitting procedure is somewhat unreliable. Powell and Morad,[3] on the other hand, observed an 8-eV threshold in their photoconductivity measurements on 1034 Å of SiO_2; again, interference effects and IPE contributions make the agreement between this value and their absorption coefficient threshold seem quite coincidental. Trukhin's[4] photoconductivity spec-

trum shows a plateau that begins only above 12 eV. We think that his results are erroneous because his samples were covered with LiF and also possibly because of inadequate shielding against secondary electrons which interfere with the current readings.

The data of Fig. 6 exhibit an approximate plateau above about 10 eV, with the structure in this region being partially due to variations in reflectance (especially near 10.5 eV) and partially due to a varying loss of carriers by recombination near the aluminum as light is absorbed closer or further from this electrode. Nevertheless, the photoyield in this region is approximately unity, as determined from an absolute intensity calibration of the detector, performed at a lower photon energy (~5.5 eV). This high yield rules out the explanation offered by Mott[8] that the currents below about 10.5 eV result from excitons which migrate to the aluminum and give up their energy to electrons in the electrode, thereby injecting some of them into the oxide (this mechanism, similarly to IPE, should have quite a low yield).

C. Photoconductivity field dependence

In view of the difficulties with the spectral dependence, more insight can be gained by examining the dependence of the photocurrents on the electrical field. This is shown by the series of curves in Fig. 7–9, for photon energies in the range of 2.6 eV $< h\nu <$ 11.1 eV which extends from below the energy barrier for IPE to above the main threshold of photoconductivity in the oxide. The curves of Fig. 7 were obtained with a visible-uv monochromator and those of Figs. 8 and 9, in the vuv monochromator. All data were taken on the same device and normalized to unity

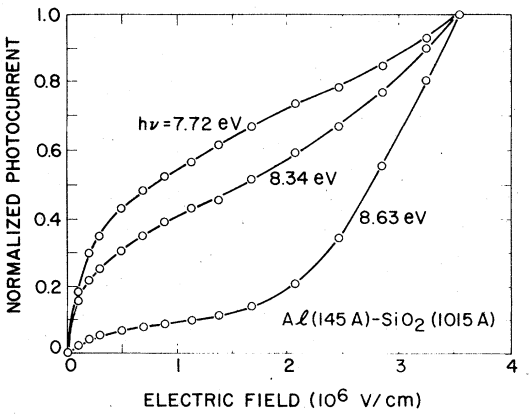

FIG. 8. Field dependence of photocurrents (Al negative) at photon energies near the absorption edge of SiO_2. At 7.72 and 8.34 eV the curves display mainly the behavior of internal photoemission (see Fig. 7 for $h\nu > 3.2$ eV), while at 8.63 eV photoconductivity (SiO_2 absorption) dominates at higher fields.

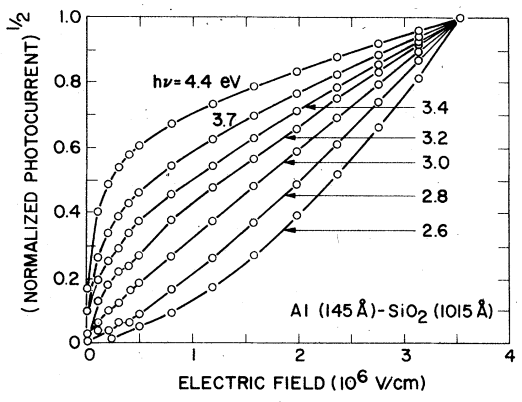

FIG. 7. Field dependence of photocurrents at various photon energies for electron injection from the Al [$-V_G$ in Fig. 1(b)] into the SiO_2. The change of curvature at about 3.2 eV is associated with the barrier height between the Al Fermi level and the SiO_2 conduction band edge (see Ref. 20). The reason for plotting (photocurrents)$^{1/2}$ is explained in Sec. II C. The curves of Figs. 7–9 are all normalized to unity.

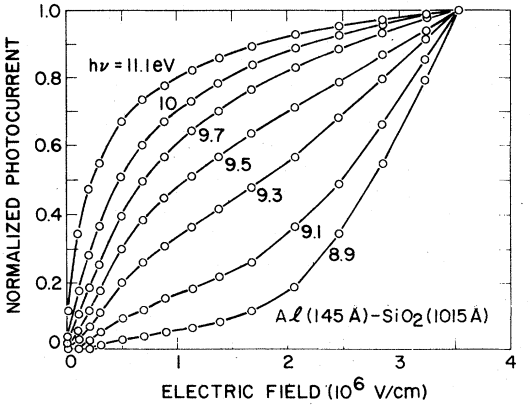

FIG. 9. Field dependence of photoconductivity (Al negative) at thermally grown SiO_2 films (amorphous) at various photon energies above the absorption edge. As in Fig. 7, we associate the change of curvature at about 9.3 eV with a "barrier height" which we identify as the SiO_2 band gap (see Secs. II C and III).

at their highest point. Measurements on samples with other oxide thicknesses gave the same results; hence the data shown are free of interference effects. The data were taken with a negative bias on the Al electrode and are discussed below. For positive bias, the following observations were made: For $h\nu > \sim 10$ eV, the currents display a complicated dependence on time and field, due to hole trapping at the interfaces.[29,42] For ~ 8.5 eV $< h\nu < \sim 10$ eV, the currents are steady and equal to the negative bias case, which is consistent with absorption mainly throughout the SiO_2 bulk. For $h\nu < \sim 8.5$ eV, the currents are smaller than for negative bias since they originate from IPE from the silicon.

The change in curvature in Fig. 7 is associated with the transition from mainly photon assisted tunneling[44] to IPE which, as has been shown by Powell,[20] occurs at $h\nu \sim \phi_B$, where ϕ_B (3.15 eV) is the barrier height between the Al Fermi level, E_F, and the oxide conduction band. In Fig. 7 the square root of the yield is plotted since in the simplest form of IPE the yield Y is given by

$$Y = A(h\nu - \phi_B + \Delta\phi)^m, \tag{1}$$

where A is a constant, $\Delta\phi$ is the image force barrier lowering, and m is a parameter which characterizes the energy distribution of the photoexcited electrons. It was previously concluded from IPE[43] and photon assisted tunneling experiments[44] that for injection from Al into SiO_2 $m \sim 2$, which corresponds to the photoexcited electrons being uniformly distributed in energy up to $E_F + h\nu$. The field rather than its square root, as predicted by the classical image force theory, has been used in the figures, since the latter tends to exaggerate the relatively unimportant low-field portion of the curves.

The transition from IPE to absorption and photoconductivity in the oxide is apparent in Fig. 8. At 7.72 and 8.34 eV the curves display a behavior which is due mainly to IPE (which increases only weakly with field); in contrast, the curve at 8.63 eV shows a sharp increase of current at higher fields, which indicates that oxide photoconductivity becomes larger than IPE.

The general behavior of the curves in Fig. 9 is similar to that of Fig. 7. This is not surprising since the separation of an electron from the hole within the oxide is not too different from the separation of an electron from the screened hole in the metal. Aside from the more subtle differences between the two cases, associated with the escape probability (dielectric constant, energy levels, etc.), the energy distribution of the photoexcited electrons is certainly different. For absorption, the distribution in energy is probably fairly narrow, which leads to a uniform distribution in the component of momentum in the direction of escape parallel to the field; this in turn gives $m = 1$ in Eq. (1). Therefore we chose to plot the yield rather than its square root in Figs. 8 and 9. Similarly to IPE (Fig. 7), where the change in curvature is associated with the barrier height, we associate the change in curvature seen in Fig. 9 with the SiO_2 band gap and deduce that $E_g \sim 9.3$ eV. This association and the 9.3-eV value are, obviously, subject to a more detailed modeling of the problem.

D. Diode experiments

A schematic illustration of the diode experiment is shown in Fig. 1(c). Shallow junctions (~ 1 μm) were fabricated by standard diffusion processes in the silicon substrate, and the oxide was grown over them. Both n/p and p/n diodes[29] were used and the oxide was unmetallized. Several oxide thicknesses in the range 450–1350 Å were used. The diode's contacts were shielded from light and from secondary electrons and the current (I) was the signal induced by the vuv light.

The diode, obviously, is a detector for photons and in principle could detect excitons too, provided that excitons diffusing in the SiO_2 can cross the Si-SiO_2 interface. Such excitons would separate in the silicon into free electrons and holes and be detected much the same as photons which are absorbed in the silicon near the Si-SiO_2 interface.

Because it is difficult to determine an absolute calibration for the diode signal, the data were normalized to the calculated transmission of the oxide in the transparent region (~ 8 eV). The diode signal was then compared with the calculated transmission for the rest of the spectrum (up to 12 eV). It was found that the diode signal was always larger by about a factor of 3–10 than that predicted from the calculated transmission in the absorbing region (over 9.8 eV). This "extra" signal was found to decay exponentially with the oxide thickness (in the range 450–1350 Å) and therefore could not be due to photoluminescence. A possible explanation of its origin is as follows: if only the initial "hot" excitons (i.e., before they recombine or relax to lower more stable energy levels) can cross the Si-SiO_2 interface, then the "extra" signal originates from a region near the Si-SiO_2 interface extended by the distance these "hot" excitons can travel. To explain the data this distance is about 150 Å. These findings merit further investigations.

The diode experiments provide, however, two useful results. They approximately confirm the transmission results of the membrane experiments and they provide an upper limit on photoluminescence. At 10.2 eV (the peak intensity of H_2 discharge) the diode with 1350 Å of SiO_2 showed a normalized signal of $\sim 10^{-4}$. Since the diode provides the best geometry for collecting photoluminescence, this value can be taken as an upper limit on photoluminescence. This result confirms the previous observation of one of us[29] that recombination is nonradiative in pure SiO_2. We point out here that PM's 5×10^{-4} limit on photoluminescence efficiency was computed erroneously because the geometrical arrangement of the membrane experiment does not allow good collection of photoluminescence. The intrinsic limit on luminescence collection is placed by the Brewster angle (total internal reflection) given by $\Theta_b = \arcsin(1/n)$, where n, the index of refraction of SiO_2, is ~1.9 (Ref. 41) for $h\nu \sim 9$ eV. The solid angle defined by Θ_b yields a photon escape efficiency from the membrane of only $(1 - \cos\Theta_b)/2 = 0.075$ which rises to 0.13 for $n = 1.5$ (in the visible).

III. DISCUSSION AND CONCLUSIONS

The presence of strong electron-hole interaction in a material like SiO_2 raises the question of whether a single value for the band gap is at all meaningful. In the amorphous form the disorder even further complicates this question. Obviously, we cannot resolve this issue here, but we point out that it is difficult to deduce the band gap solely from optical data, since excitonic and band-to-band absorption are indistinguishable in the optical spectrum. Band-structure calculations for crystalline SiO_2 which neglect the electron-hole interaction predict various values for the band gap[9-14] and, in addition, they point to a common conclusion that the onset of band-to-band absorption is weak (e.g., the one-electron joint density of state of Ref. 9, Fig. 6), and that the first spectral peak (10.45 eV) and its long tail are predominantly excitonic. Higher peaks may have substantial excitonic origins as well.[15]

More insight concerning the band-gap issue can be gained when experimental transport properties are taken into consideration. It is well known that thermally grown SiO_2 possesses a well defined and sharp conduction-band edge; evidence for this comes from the well-defined barrier observed in internal photoemission (IPE) experiments,[20,45] from the lack of thermal activation on electron mobility[46] (see discussion by Mott[8]), and from the relatively small electron trapping in dry SiO_2.[47] Our photoconductivity field dependence data (Sec. II C) display a behavior which is similar to IPE and which contains a transition energy at $h\nu = 9.3$ eV. In analogy with IPE we identify this energy as the "barrier height" for photoionization (electron-hole separation) in thermally grown (amorphous) SiO_2 and propose that this is the most direct experimental estimate of the band gap. Obviously, it is not possible to specify whether this is a direct or indirect band gap or the sum effect of both, especially since these band gaps are found to be very close in self-consistent band-structure calculations (9.2 and 9.8 eV, from Refs. 10 and 11) for α-quartz, and may be even further intermixed in amorphous SiO_2. Regarding the nature of the experimental band gap it has been implicitly identified as indirect both by DiStefano and Eastman[26] (DE) and PM[3] because they both fit portions of their data to a $(h\nu - E_g)^2$ behavior (see also Ref. 5, Sec. 4.2). DE obtain $E_g \sim 9$ eV by fitting photoconductivity data, while PM obtain $E_g \sim 8$ eV from absorption coefficient data. Our estimate of $E_g \sim 9.3$ eV is more consistent with DE, although we find that interference effects do not permit definite conclusions to be drawn from such fits.

With $E_g \sim 9.3$ eV it remains to explain the absorption tail which extends down to at least 8.4 eV (see Fig. 5) and in various silica glasses to below 8 eV.[32] In our opinion the tail is due to one or both of the following edge-broadening effects: (i) An Urbach tail which originates from excitonic absorption which is broadened by electric microfields[48] (localized fields which fluctuate both in time and space and which originate from intrinsic effects such as disorder and phonons and from extrinsic impurities). Urbach tails[49] are exponential edges usually seen below the absorption edge of insulators.[50] While an extended exponential edge is not seen for SiO_2, our absorption coefficient data (Figs. 4 and 5) show approximately exponential behavior in the range ~9.2 eV $< h\nu <$ ~10.2 eV, corresponding to about 2 decades in α.

(ii) Broadening due to band tailing at the valence-band edge. Evidence for such band tailing comes from the work on hole conduction at various temperatures in thermally grown SiO_2 films.[51,52] Mott[8] estimates the range of band tailing to be only 0.1 eV; however, Curtis and Srour[52] model their data with extended trapping in the range of ~0.5 eV.

Aside from the band-gap issue it is interesting to note that even at relatively high fields ($> 2 \times 10^6$ V/cm) the photocurrents of Fig. 9 do not saturate. This indicates that an appreciable fraction of the electron-hole pairs are not dissociated

by the applied field, and by definition remain then as excitons. The field dependence of Fig. 9 cannot be attributed to any other phenomena, such as trapping of free carriers (Schubweg effects) because of the low trapping of both electrons and holes in the bulk of dry SiO_2 (Ref. 47) (trapping of holes is strong near the interfaces only[53]); neither can it be explained by recombination of free (separated) electron and holes because of their low volume densities (~10^4 and ~10^{10} cm^{-3} assuming mobilities of ~20 and ~10^{-5} $cm^2/V\,sec$ for electrons and holes at room temperature, respectively; with a current of 10^{-7} A/cm^2 and a field of 10^6 V/cm). The excitons do not recombine radiatively (see Sec. II D) and some general features of their lifetime before self-trapping have been discussed by Mott and Stoneham.[54] We have previously interpreted our findings of charging effects in MOS structures illuminated by vuv light with the Al electrode biased negatively as evidence for diffusion of such excitons from near the Al-SiO_2 interface to the Si-SiO_2 interface.[1,35] However, we have found recently that the effect increases in samples treated in water, which raises an alternative possibility that the effect can be explained by diffusion of water-related species (such as hydrogen). This issue is presently unresolved.

In summary, extensive transmission and photoconductivity data for thin thermally grown SiO_2 films have been presented and discussed. Threshold determination from spectral data has been criticized, and it is proposed that a band gap of 9.3 eV for SiO_2 can be extracted from the field dependence of photoconductivity.

ACKNOWLEDGMENTS

One of us (ZAW) is indebted to D. J. DiMaria for critical discussions and for experimental help in the IPE measurements, and to H. R. Philipp for supplying detailed tables of optical constants for SiO_2, Si, and Al. For sample preparation we are grateful to K. E. Belcher, J. W. Kuran, E. J. Petrillo, H. Pinckney, and S. K. Tharas, and for experimental assistance to J. A. Calise, J. J. Donelon, A. Marx, and F. L. Pesavento. This work was supported in part by the Defense Advanced Research Projects Agency, the Department of Defense, and monitored by the Deputy of Electronic Technology under Contract No. F19628-76-C-0249.

APPENDIX

The transmission (normal incidence) of a thin film of thickness d and complex index of refraction $n-ik$, suspended in vacuum, is given by[55]

$$T = a/(b_1 e^{\sigma} + b_2 e^{-\sigma} + b_3 \cos\gamma + b_4 \sin\gamma),$$

where

$$\sigma = \frac{4\pi k d}{\lambda}, \quad \gamma = \frac{4\pi n d}{\lambda}, \quad \lambda\text{: vacuum wavelength;}$$

$$a = 16(n^2 + k^2),$$

$$b_1 = [(1+n)^2 + k^2]^2,$$

$$b_2 = [(1-n)^2 + k^2]^2,$$

$$b_3 = 2[4k^2 - (n^2 + k^2 - 1)^2],$$

$$b_4 = 8k[n^2 + k^2 - 1].$$

The absorption coefficient α was calculated from

$$\alpha \equiv \frac{4\pi k}{\lambda} = \frac{1}{d} \ln\left[\frac{1}{b_1}\left(\frac{a}{T} - b_2 e^{-\sigma} - b_3 \cos\gamma - b_4 \sin\gamma\right)\right].$$

This equation was solved by iteration with Philipp's[41] k values as the initial guess, and his n values as constants.

*Present address: Electrical Engineering Dept., Technion, Haifa 32000, Israel.
[1]Z. A. Weinberg and G. W. Rubloff, in *The Physics of SiO_2 and its Interfaces*, edited by S. T. Pantelides (Pergamon, New York, 1978), p. 24.
[2]D. A. Stephenson and N. J. Binkowski, J. Non-Cryst. Solids 22, 399 (1976).
[3]R. J. Powell and M. Morad, J. Appl. Phys. 49, 2499 (1978).
[4]A. N. Trukhin, Phys. Status Solidi B 86, 67 (1978).
[5]D. L. Griscom, J. Non-Cryst. Solids 24, 155 (1977).
[6]S. T. Pantelides, Comments Solid State Phys. 8, 55 (1977).
[7]S. T. Pantelides, *The Physics of SiO_2 and its Interfaces* (Pergamon, New York, 1978).
[8]N. F. Mott, Adv. Phys. 26, 363 (1977).
[9]N. F. Mott, in *The Physics of SiO_2 and its Interfaces*, edited by S. T. Pantelides (Pergamon, New York, 1978), p. 1.
[10]J. R. Chelikowsky and M. Schlüter, Phys. Rev. B 15, 4020 (1977).
[11]M. Schlüter and J. R. Chelikowsky, Solid State Commun. 21, 1123 (1977).
[12]P. M. Schneider and W. B. Fowler, Phys. Rev. Lett. 36 (425) 1976.
[13]E. Calabrese and W. B. Fowler, Phys. Rev. B 18, 2888 (1978).
[14]S. Ciraci and I. P. Batra, Phys. Rev. B 15, 4923 (1977).
[15]S. T. Pantelides, in *The Physics of SiO_2 and its Interfaces*, edited by S. T. Pantelides (Pergamon, New York, 1978), p. 80.
[16]W. Groth and H. V. Weyssenhoff, Z. Naturforsch. A 11, 165 (1956).

[17]R. Williams, Phys. Rev. 140, A569 (1965).
[18]A. M. Goodman, Phys. Rev. 152, 780 (1966).
[19]R. Williams, *Semiconductors and Semimetals*, edited by R. K. Willardson and A. C. Beer (Academic, New York, 1970), Vol. 6, p. 97.
[20]R. J. Powell, J. Appl. Phys. 41, 2424 (1970).
[21]E. Loh, Solid State Commun. 2, 269 (1964).
[22]K. Platzöder, Phys. Status Solidi 29, K63 (1968).
[23]H. R. Philipp, Solid State Commun. 4, 73 (1966).
[24]H. R. Philipp, J. Phys. Chem. Solids 32, 1935 (1971).
[25]R. J. Powell and G. J. Derbenwick, IEEE Trans. Nuc. Sci. 18, 99 (1971).
[26]T. H. DiStefano and D. E. Eastman, Solid State Commun. 9, 2259 (1971).
[27]H. Ibach and J. E. Rotw, Phys. Rev. B 10, 710 (1974).
[28]Y. P. Zakis, A. N. Trukhin, and V. P. Khimov, Sov. Phys. Solid State 15, 149 (1973).
[29]Z. A. Weinberg, Appl. Phys. 27, 437 (1975).
[30]R. C. Hughes, Phys. Rev. B 15, 2012 (1977).
[31]I. P. Kaminow, B. G. Bagley, and C. G. Olson, Appl. Phys. Lett. 32, 98 (1978).
[32]A. Appleton, T. Chiranjivi, and M. Japaripour-Ghazvini, in *The Physics of SiO_2 and its Interfaces*, edited by S. T. Pantelides (Pergamon, New York, 1978), p. 94.
[33]G. H. Sigel, Jr., J. Non-Cryst. Solids 13, 372 (1973/74).
[34]E. Lell, N. J. Kreidl, and J. R. Heusler, Prog. Ceramic. Sci. 3, 1 (1966).
[35]Z. A. Weinberg and G. W. Rubloff, Appl. Phys. Lett. 32, 184 (1978).
[36]J. A. R. Samson, *Techniques of Vacuum Ultraviolet Spectroscopy* (Wiley, New York, 1967).
[37]C. W. Wilmsen, E. G. Thompson, and G. H. Meissner, IEEE Trans. Electron Devices 19, 122 (1971).
[38]K. E. Petersen, Appl. Phys. Lett. 31, 521 (1977).
[39]R. M. Finne and D. L. Klein, J. Electrochem. Soc. 114, 965 (1967).
[40]E. Bassous and E. F. Baran, J. Electrochem. Soc. 125, 1321 (1978).
[41]We used values kindly provided in table form by H. R. Philipp. For the published data see Refs. 23 and 24 above.
[42]R. J. Powell, J. Appl. Phys. 46, 4557 (1975).
[43]P. M. Solomon and D. J. DiMaria (private communication).
[44]Z. A. Weinberg and A. Hartstein, Solid State Commun. 20, 179 (1976).
[45]A. Hartstein, Z. A. Weinberg, and D. J. DiMaria, in *The Physics of SIO_2 and its Interfaces*, edited by S. T. Pantelides (Pergamon, New York, 1978), p. 51.
[46]R. C. Hughes, Phys. Rev. Lett. 30, 1333 (1973).
[47]D. J. DiMaria, in *The Physics of SiO_2 and its Interfaces*, edited by S. T. Pandelides (Pergamon New York, 1978), p. 160.
[48]J. D. Dow, in *Optical Properties of Highly Transparent Solids*, edited by S. S. Mitra and B. Bendow (Plenum, New York, 1975), p. 131.
[49]F. Urbach, Phys. Rev. 92, 1324 (1953).
[50]J. Tauc, in *Optical Properties of Highly Transparent Solids*, edited by S. S. Mitra and B. Bendow (Plenum, New York, 1975), p. 245.
[51]F. B. McLean, G. A. Ausman, Jr., H. E. Boesch, Jr., and M. McGarity, J. Appl. Phys. 47, 1529 (1976).
[52]O. L. Curtis, Jr. and J. R. Srour, J. Appl. Phys. 48, 3819 (1977).
[53]D. J. DiMaria, Z. A. Weinberg, and J. M. Aitken, J. Appl. Phys. 48, 898 (1977).
[54]N. F. Mott and A. M. Stoneham, J. Phys. C 10, 3391 (1977).
[55]G. Hass and L. Hadley, *American Institute of Physics Handbook*, 3rd ed. (McGraw-Hill, New York, 1972), p. 6–120.

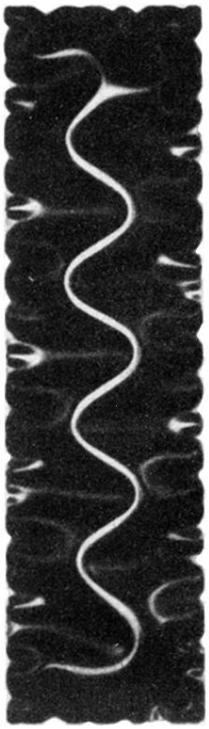

FIG. 2. Photograph of a membrane measuring 1.0 ×0.25 mm, showing the sinusoidal pattern produced by microscope light interference in the slightly wrinkled SiO_2 film.